Sensors and Actuators B 242 (2017) 1035–1042

Contents lists available at ScienceDirect

Sensors and Actuators B: Chemical

journal homepage: www.elsevier.com/locate/snb

Zn(II)-selective and sensitive fluorescent chemosensor based on steric constrains and inhibition of ESIPT

Caixia Yuan[a,b,*], Shiyang Li[a], Yanbo Wu[a,b], Liping Lu[a,**], Miaoli Zhu[a,b]

[a] Institute of Molecular Science, Key Laboratory of Chemical Biology and Molecular Engineering of the Education Ministry, Shanxi University, Taiyuan, Shanxi 030006, PR China

[b] Key Laboratory of Materials for Energy Conversion and Storage of Shanxi Province, Institute of Molecular Science, Shanxi University, Taiyuan, Shanxi 030006, PR China

ARTICLE INFO

Article history:
Received 31 July 2016
Received in revised form
22 September 2016
Accepted 24 September 2016
Available online 27 September 2016

Keywords:
Naphthoxazole
Zn(II)
Fluorescence
Chemosensor
Theoretical calculation
ESIPT

ABSTRACT

A new naphthoxazole-derived probe, 2-(2-Hydroxyphenyl)-naphtho[1,2-*d*]oxazole-5-sulfonate (HL), was conveniently synthesized and characterized. The presence of Zn^{2+} caused an obvious fluorescence enhancement at 458 nm upon excitation at 391 nm, which could be distinguished with the naked eye under a UV lamp. Remarkably, the compound exhibited excellent selective and sensitive response to Zn^{2+} over other common cations with a micromolar limit of detection (0.69 μM) in DMSO/HEPES (v/v, 1:1) buffer. The results from absorption spectra, ^{1}H NMR, ESI–MS, density functional theory (DFT) calculations, and pH effect, implied that during the process of complexation, the fluorescence intensity was enhanced by the inhibition of the excited state intramolecular proton transfer (ESIPT) in free HL and the formation of a large π-electron conjugation system. The steric hindrance effect from a hydrogen atom on naphthoxazole determined the selectivity of Zn^{2+} over other metal ions. The most appropriate environments for the detection of Zn^{2+} were neutral and weak alkali. In addition, the probe of detecting the Zn^{2+} has been evaluated with relatively lower toxicity in living MCF7 cell, suggesting the practical application in physiological system.

1. Introduction

As one of the essential micronutrients in human body, the divalent zinc ion plays the crucial role in many physiological processes, such as DNA replication and repair, gene expression and cellular metabolism [1–3]. Therefore, detection of Zn^{2+} has attracted considerable attentions of chemists, biologists, and physiologists in recent years. The technique of fluorescence has been demonstrated to be a powerful tool to sense various analytes with its high sensitivity and simplicity [4] and a large number of fluorescent sensors were designed to detect heavy and transition metal ions, which was found to be potentially useful in the fields including chemistry, environment, biology and medicine [5–11]. Over the past few decades, numerous fluorescent chemosensors for the detection of Zn^{2+} have been developed based on aromatic heterocyclic fluorophores, such as quinoline [12], coumarin [13], furan [14], benzoxazole [15], triazole [16], benzoimidazole [17] and pyrazoline [18] *etc*. Nevertheless, the design of facile, easy to synthesize, low toxic Zn^{2+}-selective probes is still a challenge. Specifically, the discrimination of Zn^{2+} from its heavy congeners Cd^{2+} and Hg^{2+} is generally difficult, because they have the similar shell electronic structures and exhibit similar bonding preferences.

Naphthoxazole derivatives are considered as an important class of heterocyclic compounds since they exhibit broad spectrum of biological and photochromatic activities [19,20]. It is reported that 2-subsitituted naphthoxazole is a major subunit occurring in some natural products [21], which indicates that naphthoxazole derivatives are environment-friendly and low-toxic to the human body. These desired properties render them potentially useful fluorescent probe for detecting metal ion in physiological systems.

In this work, a simple naphthoxazole derivative probe was designed and synthesized. The new probe showed the excited-state intramolecular proton transfer (ESIPT) processes, one of the most common photophysical phenomenon that occured in the heterocyclic molecules involving the transfer of a hydroxyl proton to an adjacent imine nitrogen [22]. The inhibition of ESIPT by the coordi-

* Corresponding author at: Institute of Molecular Science, Key Laboratory of Chemical Biology and Molecular Engineering of the Education Ministry, Shanxi University, Taiyuan, Shanxi 030006, PR China.
** Corresponding author at: Institute of Molecular Science, Key Laboratory of Chemical Biology and Molecular Engineering of the Education Ministry, Shanxi University, Taiyuan, Shanxi 030006, PR China.
E-mail addresses: cxyuan@sxu.edu.cn (C. Yuan), luliping@sxu.edu.cn (L. Lu).

http://dx.doi.org/10.1016/j.snb.2016.09.149
0925-4005/

nation to the metal ions often leads to the obvious changes in the spectra and thus it can be employed to generate the fluorescent response for detecting the metal ions. Simultaneously, the naphthalene part of the probe has a blocking effect for the bidentate coordination ability that may be useful to selective detecting the metal ions [23]. As expect, we found that the probe could selectively and sensitively detect Zn^{2+} by the specific coordination to Zn^{2+} with a simultaneous inhibiting ESIPT effect, which was demonstrated by the fluorescence studies in combination with ^1H NMR, ES–MS analysis, density functional theory (DFT) calculations, and pH effect. Remarkably, such a compound is low toxic to the living cell and also sensitive to Zn^{2+} in it, suggesting the practical application for the detection of Zn^{2+} in physiological system.

2. Experimental

2.1. Materials and general methods

Unless specially noted, all chemicals were purchased from commercial suppliers without further purification. Double distilled water was used to prepare all aqueous solutions. Elemental analyses were performed on VARI-EL elemental analyzer. IR spectra in KBr discs were recorded using Shimadiu-FTIR-8300 Spectrophotometer in the range of 4000–400 cm^{-1}. ESI mass spectra were acquired on a Triple TOF^{TM} 5600$^+$ system. ^1H NMR spectra were performed on a Bruker 600 MHz instrument. The fluorescence and electronic spectra were obtained using Cary 50 and Cary Eclipse Spectrophotometer (Varian, USA) at room temperature, respectively. Fluorescence images of MCF7 cells were performed with a confocal laser scanning microscope with model LSM-880.

2.2. Synthesis of naphthoxazole derivative HL

1-Amino-2-naphthol-4-sulforic acid (1 mmol, 0.2390 g) was suspended in 40 mL of absolute methanol in a flask and a 150 μL of triethylamine (1 mmol,) was added to the reactor. The suspension was heated to reflux until the solution became clear and then 5-chlorosalicylaldehyde (1 mmol, 0.2551 g) in 10 mL of absolute ethanol was added dropwise to this mixture. Dark yellow precipitates were obtained after the solution was further refluxed for 4 h. The solid powder was isolated by vacuum filtration, washed with distilled water, ethanol, and diethyl ether, respectively, and dried in vacuo. Yield: 65%. ^1H NMR (600 MHz, DMSO-d_6): δ = 11.25 (s, 1H,), 9.05 (d, 1H), 8.54 (d, 1H), 8.34 (s, 1H), 8.10 (s, 1H), 7.76 (m, 1H), 7.66 (m, 1H), 7.56 (m, 1H), 7.21 (d, 1H). Anal. Calcd. for $C_{17}H_9ClNO_5S{\cdot}C_6H_{16}N$: C 57.92, H 5.28, N 5.87%. Found: C 58.03, H 5.21, N 5.86%. FT-IR (ν/cm^{-1}):3444, 1633, 1584, 1536, 1483, 1449, 1206, 1188, 1055.97, 754, 654. ESI–MS: m/z calcd (%) for $[C_{17}H_{11}ClNO_5S]^+$: 375.78; found 376.00 (100%). Λ_m (H_2O) 92.4 μS/cm. Dark yellow block crystals were received by slow evaporation of the reaction solution at room temperature for 2 weeks.

2.3. X-ray crystallography

Diffraction data for the probe HL were collected in Beijing Synchrotron Radiation Facility (BSRF) beamline 3W1A, which was mounted with a MARCCD-165 detector (λ = 0.7200 Å) with storage ring working at 2.5 Ge V. Data were collected by the MARCCD program and processed using HKL 2000 [24] at the 100 K. The structure was solved by direct methods and refined by the full-matrix least-squares technique using the SHELXS-97 [25]. The crystallographic data and structure refinement parameters for the compound are showed in Table S1 (supporting materials). The CIF file for HL was deposited in the Cambridge structure Database with CCDC no.1495716, obtained free of charge *via* www.ccdc.cam.ac.uk/conts/retrieving.html.

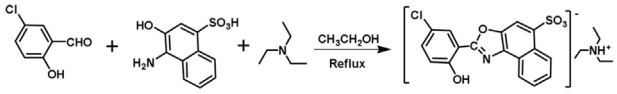

Scheme 1. Synthesis of the probe HL.

2.4. UV–vis and fluorescence spectra studies

A stock solution of HL (0.1 M) was prepared in DMSO. Stock solutions of the metal ions (0.1 M) were prepared in double distilled water. The effects on the addition of different metal ions to HL were investigated in the DMSO/HEPES buffer solution (10 mM, pH = 7.2; 1:1(v/v)) through UV–vis and Fluorescence measurements at the room temperature. The limit of detection (LOD) was calculated based on the standard deviation of the response (SD) and the slope of the calibration curve (S) at levels approximating the LOD according to the formula: (LOD) = 3(SD)/S.

2.5. DFT calculations

The solvation effect was considered for all calculations by using the polarizable continuum model (PCM). The ground state structures were optimized and vibrational frequencies were analyzed at B3LYP/6-31G(d) level. The excited state structures were considered with the time-dependent (TD) procedure. The UV–vis spectra were simulated by the single point TD-B3LYP/6-31G(d) calculations at the ground state optimized structures and the fluorescence spectra were calculated by the geometry optimization at excited state potential energy surfaces with the ground state optimized structures as the starting points at B3LYP/6-31G(d) level. To compare the relative energies of enol and keto isomers at both ground and excited states, the energies were improved by the single point calculations at B3LYP/6–311 + G(d,p) level based on the B3LYP/6-31G(d) optimized structure. All calculations were performed using Gaussian 09 package.

2.6. Methods for biological application

MCF7 cells were cultured in DMEM (Dulbecco's Modified Eagle Medium) medium supplemented with penicillin/streptomycin (100 units/mL) and 10% fetal bovine serum (FBS) and grown at 37 °C in a humidified atmosphere in the presence of 5% CO_2. Cells were treated with the probe HL (10 μM) in PBS buffer (1% DMSO, pH = 7.5) for 2 h. At the end of 2 h, the cells were then incubated with Zn^{2+} (10 μM) for further 2 h. The cells were washed with PBS buffer three times. And the living cell images were captured through a confocal laser scanning microscope. The viability of MCF7 cells in the presence of the probe HL was determined by the 3-[4,5-Dimethylthiazo-2-*yl*]-2,5-diphenpyltetra-zolium bromide (MTT) assay.

3. Results and discussion

3.1. Synthesis and characterization of the probe HL

Previously, we had facilely synthesized several Schiff-base compounds by the condensation connection between the salicylaldehyde and aromatic amine or triazole amine [26–28]. In this work, a new naphthoxazole derivative (HL) was further prepared by one step condensation of a polycyclic aromatic amine (1-amino-2-naphthol-sulfonic acid) and 5-chlorosalicylaldehyde in the presence of triethylamine (Scheme 1). The probe was con-

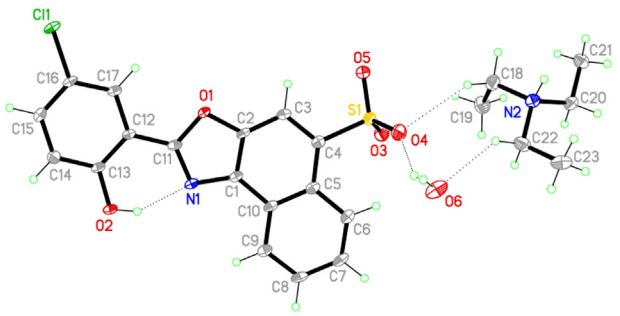

Fig. 1. Crystal structure diagram of the probe HL with 50% probability displacement ellipsoids, dot lines for H bondings.

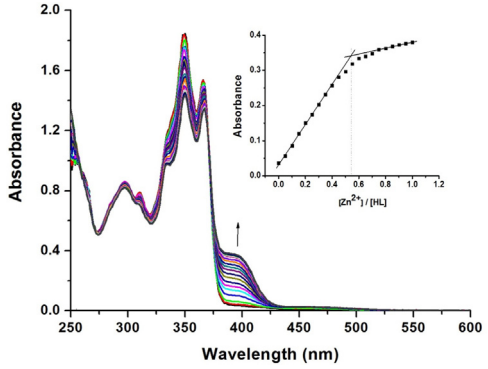

Fig. 2. Absorption titration of the probe HL (2 mL, 0.1 mM) with Zn^{2+} (0–0.1 mM) in DMSO/HEPES buffer (pH = 7.2, v:v = 1:1) at room temperature. Inset shows absorption *vs.* $[Zn^{2+}]/[HL]$ (λ = 391 nm).

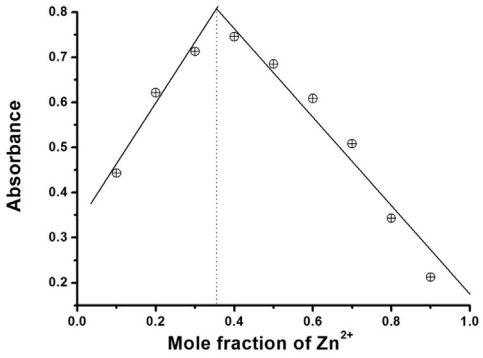

Fig. 3. Job's plot of Zn-L complex in HEPES buffer (pH = 7.2, DMSO/HEPES = 1:1). The total molar concentration of HL and Zn^{2+} is 5 mM, λ = 391 nm.

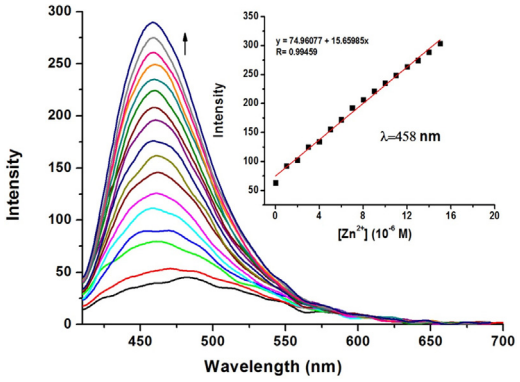

Fig. 4. Fluorescence spectra of sensor HL (1 μM) on addition of different amount of Zn^{2+} in DMSO/HEPES (v/v, 1:1, pH = 7.4). Inset: Fluorescence intensity at 458 nm changes on incremental addition of Zn^{2+}(0 ~ 15 μM).

firmed by elemental analysis, IR spectroscopy, ^{1}H NMR, ESI–MS (Figs. S1–S6, supporting materials), and single crystal X-ray crystallography (Fig. 1). The X-ray crystallographic structure reveals that the probe HL crystallizes in the $P2_1/c$ space group of the monoclinic crystal system. The phenol oxygen and naphthoxazole nitrogen atoms can provide suitable chelate coordination site in the presence of metal cations. Obviously, there is an stronger intramolecular hydrogen bonding between the phenol (O2) and imino nitrogen (N1) atoms of naphthoxazole with a distance of 2.662 Å, which is necessary for occurrence of the desired ESIPT process [29].

3.2. UV–vis absorption studies

The *UV–vis* absorption spectral properties of the probe HL with or without metal ions (such as K^+, Na^+, Ca^{2+}, Mg^{2+}, Al^{3+}, Ba^{2+}, Fe^{3+}, Co^{2+}, Ni^{2+}, Cu^{2+}, Mn^{2+}, Cr^{3+}, Cd^{2+}, Hg^{2+}, and Zn^{2+}) were investigated in DMSO/HEPES buffer (pH = 7.2, v/v = 1:1) (Fig. S7, supporting materials). The absorption spectrum of the probe HL showed the two main low energy bands at 349 and 365 nm, respectively. The spectral pattern of HL does not exhibit any significant change on adding majority of metal ions except Zn^{2+}. Therefore, the UV–vis absorption titrations were carried out by gradual addition of Zn^{2+} to the solution of probe HL. As shown in Fig. 2, the absorption peaks of HL decrease gradually with additions of Zn^{2+}, whereas a new absorption peak at 391 nm appears and gradually increases, which implies the formation of Zn complex with the ligand.

For better understanding the interaction of the probe HL with Zn^{2+}, Job's plot analysis was conducted. The results show the absorbance intensity of the solution reaches maximum when the mole fraction of Zn^{2+} is about 0.35 (Fig. 3), which indicates a 2:1 complexation stoichiometry between HL and Zn^{2+}. The binding stoichiometry was further confirmed by ESI–MS spectrometry analysis. The positive-ion mass spectrum of the probe HL solution in the presence of Zn^{2+} (1 equiv) exhibits a prominent peak at m/z = 416.36, which is assignable to $\{[Zn(C_{17}H_9ClNO_5S)_2] + 2H^+ + H_2O\}^{2+}$ species (cald.416.47) (Fig. S6, supporting materials).

3.3. Fluorescence emission studies

The fluorescence properties of HL (1.0 μM) for the titration of Zn^{2+} were studied in DMSO/HEPES (pH = 7.2, 1:1 v/v) system. As shown in Fig. 4, the probe shows that a weak fluorescence emission at 485 nm when it is excited at 391 nm. With gradual increase in the Zn^{2+} concentration (1 ~ 15 μM), the emission intensity of the probe HL increases continuously and the emission maximum shifts from 485 to 458 nm. It is noteworthy that the fluorescence changes induced by Zn^{2+} exhibits good linear relationships (Fig. 4, inset), which means that the probe HL is suitable for quantitative detection of Zn^{2+}. The limit of detection calculated according to the formula ((LOD) = 3(SD)/S) is 6.9×10^{-7} M, which is lower than most of the reported zinc ion chemosensors based on inhibiting ESIPT process (Table S2, supporting materials) [30–35]. This low limit of detection indicates that the probe HL may be an efficient fluorogenic chemosensor for Zn^{2+} recognition.

The comparative studies among the addition of 20 μM of familiar metal ions such as Zn^{2+}, K^+, Na^+, Ca^{2+}, Mg^{2+}, Al^{3+}, Ba^{2+}, Fe^{3+}, Co^{2+}, Ni^{2+}, Cu^{2+}, Mn^{2+}, Cr^{2+}, Cd^{2+}, and Hg^{2+}, respectively, were performed. As shown in Fig. 5, only the addition of Zn^{2+} can greatly increase the intensity and also lead to the blue shift of fluorescence of HL. Remarkably, an obviously blue emission of the solution can be easily visualized by the naked eye under a UV lamp at 365 nm (Fig. 5, Inset). Furthermore, the competitive experiments were performed for HL (1 μM) in the presence of Zn^{2+} (10 μM) mixed with

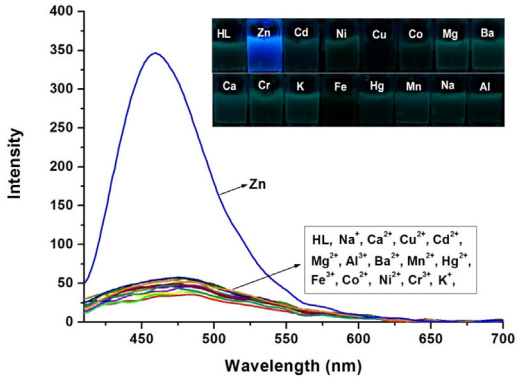

Fig. 5. Fluorescence (λ_{ex} = 391 nm) responses of HL respectively upon the addition of several metal ions in DMSO/HEPES (v/v = 1:1) at emission slit 5 nm. Inset: a color change photograph for Zn^{2+} and the other metal ions under illumination with a 365 nm UV lamp.

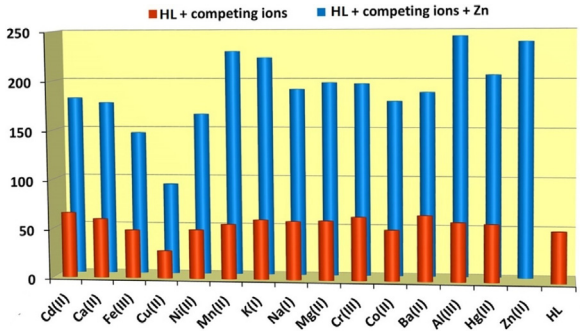

Fig. 6. Fluorescence intensity of HL and its complexation with Zn^{2+} in the presence of various metal ions in DMSO/HEPES (v/v, 1:1), Red bar: HL (1 μM) and HL with 10 equiv. of competing ions, Blue bar: 1 μM of HL, 10 μM of competing ions and Zn^{2+} (λ_{ex} = 391 nm, λ_{em} = 458 nm, slit widths: 5 nm/5 nm). (For interpretation of the references to colour in this figure legend, the reader is referred to the web version of this article.)

other interfering metal ions (10 μM) to evaluate the selectivity of the sensor. As shown in Fig. 6, the competitive metal ions shows the weaker response, and the coexisting metal ions except Cu^{2+} do not significantly interfere with the intensity of emission Zn-L system, while for the presence of Cu^{2+}, the moderate decrease in the intensity of fluorescence can be observed, which indicates that Cu^{2+} may compete with Zn^{2+} for binding with HL. Nevertheless, the overall results reveal that the probe HL shows a good selectivity towards Zn^{2+}.

The reversibility of the recognition process of the probe HL was examined by adding a bonding agent, ethylenediaminetetraacetic acid disodium salt (Na_2H_2EDTA) to the mixture solution of the probe HL and Zn^{2+} (10 equiv of HL). As shown in Fig. 7, the fluorescent peak at 458 nm is immediately quenched when EDTA is added the Zn-L system. But when more Zn^{2+} is added to the solution, the fluorescence is recovered to about a half again. The results show that the probe HL is reversible to a certain extent. The reversibility is important for developing the resumable fluorescent sensor for Zn^{2+} in the presence of most competing metal ions.

3.4. ^1H NMR binding studies

To further insight into the binding event of HL with Zn^{2+}, ^1H NMR spectra of L (in DMSO-d_6) in the absence and presence of Zn^{2+} were compared (Fig. 8). For HL, the shift of proton at 11.25 ppm can be assigned to the H on hydroxyl, which is involved in the intramolecular hydrogen bond (O—H ···N,) [13]. And a singlet at 8.34 ppm corresponds to H-f of the naphthalene ring. The accurate assign-

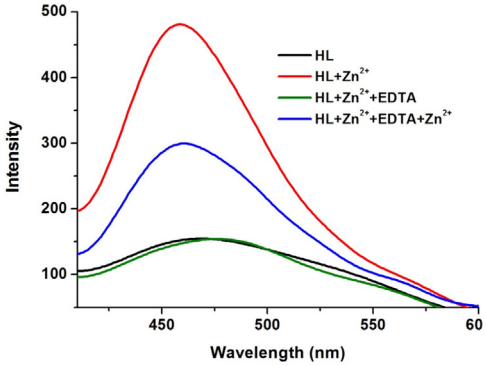

Fig. 7. Fluorescence intensity of HL with Zn^{2+} ions and EDTA in DMSO-HEPES solution (v/v, 1:1).

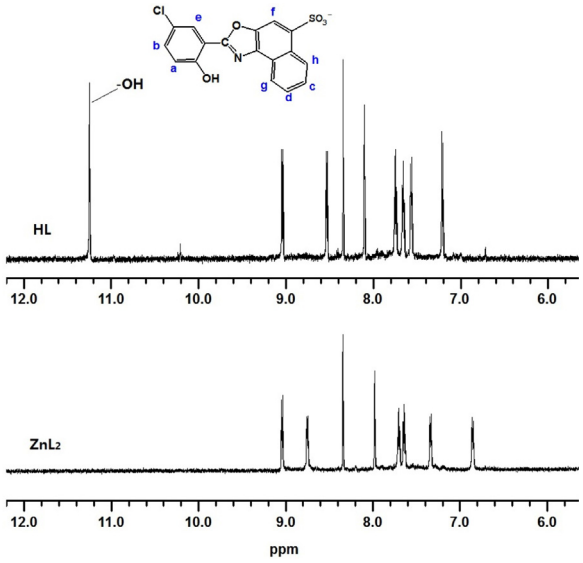

Fig. 8. ^1H NMR spectra of HL and Zn-L complex in DMSO-d_6.

ments of the other protons for HL in DMSO-d_6 were performed through the correlations in ^1H-^1H COSY spectrum (Fig. S4, supporting materials). The COSY spectrum shows the cross-peak between the signals at 7.21 and 7.56 ppm. The doublet at 7.21 (J = 8.4, coupling of H-a with H-b) and the doublet of doublets at 7.56 ppm correspond to H-a and H-b respectively, where H-a appears more upfield as compared to H-b due to the effect of OH group on adjacent carbon. A proton H-e appears as a weak doublet at 8.10 ppm due to the long-range coupling of H-e with H-b (J = 2.4 Hz). Similarly, the other three cross-peaks between the signals at 7.76 and 8.54 ppm, the signals at 7.66 and 9.05 ppm, and those at 7.76 and 7.66 ppm also are observed in the COSY spectrum, indicating that the four protons corresponding to these signals can be assigned in the naphthalene ring. Of them, the doublet at 9.05 ppm corresponds to H-h of the naphthalene ring due to the effect of SO_3 group adjacent carbon. So the proton peaks at 8.54, 7.76, and 7.66 ppm should be assigned to H-g, H-d, H-c. Upon addition of Zn^{2+}, the loss of peak at 11.25 ppm is immediately observed and doublet of H-a upfield shifted from 7.21 ppm to 6.85 ppm, which suggests that the hydroxyl might lose the H atom and corresponding oxygen atoms might coordinate to Zn ion. Moreover, the doublet at 8.54 ppm downfield shifts to 8.75 ppm, while the shifts of other aromatic protons show hardly change, indicating that the imine nitrogen in oxazole is bonded to Zn ion.

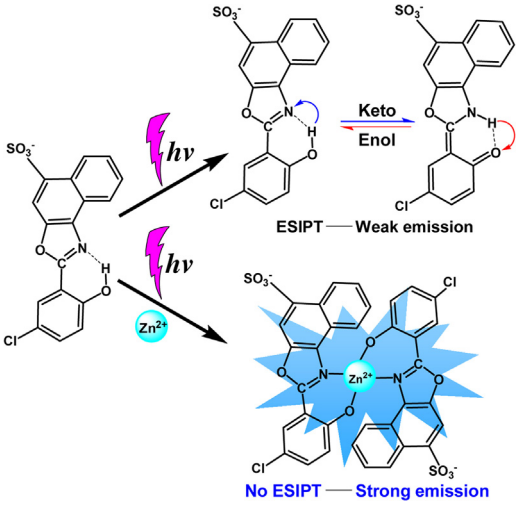

Scheme 2. The ESIPT pathway of the probe HL and the proposed mechanism for detection of Zn^{2+} by HL.

3.5. Fluorescence recognition mechanism

Why did the HL show a weak fluorescence emission but the fluorescence remarkably enhance in the presence of Zn^{2+}? We reason that the intensity of fluorescence emission depends mainly on the ESIPT process. As depicted in Scheme 2, the probe HL contains a phenolic hydroxy group at the 2-position, which may form a hydrogen bond with the nitrogen atom on naphtha[1,2-*d*] oxazole ring. The formation of such hydrogen bond can be confirmed by ^{1}H NMR spectrum and X-ray crystallography. At excited state, it is common that the proton will hop between enol-imine (O—H···N) and keto-amine (O···H—N) forms, i.e. the so-called ESIPT process (see upper part of Scheme 2). The ESIPT may lead to the weak fluorescence of the HL [36]. Upon stable chelation with Zn^{2+} and simultaneous loss of hydroxyl proton, the ESIPT process in corresponding probe is prevented, resulting in significant enhancement of the fluorescence(see lower part of Scheme 2). Moreover, the binding of Zn^{2+} with the probe will form a little more rigid large π-electron conjugation system, which will aid in the fluorescence enhancement of the probe.

Moreover, how did the probe recognize Zn^{2+} from its congeners Cd^{2+} and Hg^{2+}? Our studies suggest that it comes from the peculiar geometry of the probe. With regard to Zn^{2+}, it has the electron configuration of $3d^{10}$, which makes the tetrahedral coordination to be a favorable binding manner because it can support the stable 18-electron shell structure around Zn^{2+}. Based on this feature, Zn^{2+} ion can be distinguished from many other transition metals, which do not favor the tetracoordination. Moreover, though Cd^{2+} and Hg^{2+} have the electron configuration of $4d^{10}$ and $5d^{10}$, similar to Zn^{2+} with filled d-configurations, their ionic radii (C.N.4) are obviously larger than that of Zn^{2+} (0.78, 0.90 versus 0.60 Å) [37], which can be used to discriminate Zn^{2+} from Cd^{2+} and Hg^{2+} *via* the geometrical effect [38]. As shown in Fig. 1, H atom on C9 brings strong steric hindrance when a metal atom is coordinated by the hydroxyl O and naphthaoxazole N, which will restrict the large metal ions to enter the bidentate site of the probe. Then, it is understandable that only the presence of Zn^{2+} can enhance the fluorescence because Cd^{2+} and Hg^{2+} are obviously larger in size than Zn^{2+} and they are unsuitable for the formation of stable coordination complex with the probe.

3.6. Theoretical studies

To verify the proposed mechanism of recognition, we performed the DFT calculations. As shown in Fig. 9, at the ground electronic state, the B3LYP/6–311 + G(d,p) single point calculations on the B3LYP/6-31G(d) optimized structures (B3LYP/6–311 + G(d,p)//B3LYP/6- 31G(d)) reveal that the enol form isomer is 0.41 eV (9.6 kcal/mol) lower in energy than the keto form isomer. Such a large energy difference indicates that HL exists mainly in enol form. However, at the first excited state, the TD-B3LYP/6–311 + G(d,p)//TD-B3LYP/6-31G(d) calculations reveal that the enol form isomer is only 0.03 eV (0.7 kcal/mol) lower in energy

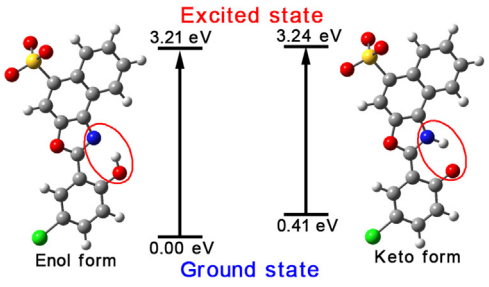

Fig. 9. The structures and relative energies of enol and keto forms of HL at both ground and excited states. The energy of enol form at ground state is set as zero.

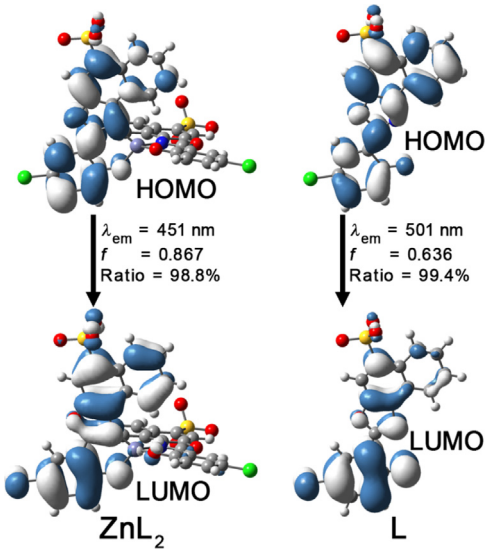

Fig. 10. The fluorescent emission mechanism for ZnL_2 complex and deprotoned probe (L). "λ_{em}", "*f* ", "Ratio" denote the wavelength of emission, the oscilator strength, and the ratio for corresponding transition in the concerned exicted state.

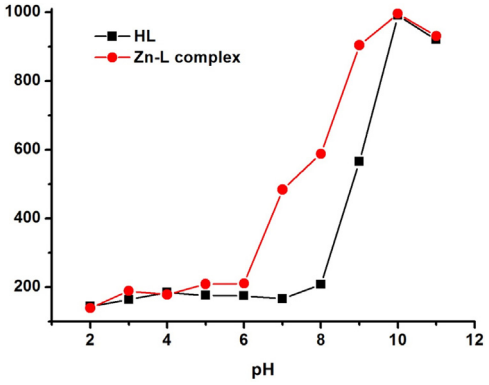

Fig. 11. Effect of pH on the maximum emission peak of HL and Zn-L complex in DMSO/HEPES (v/v, 1:1).

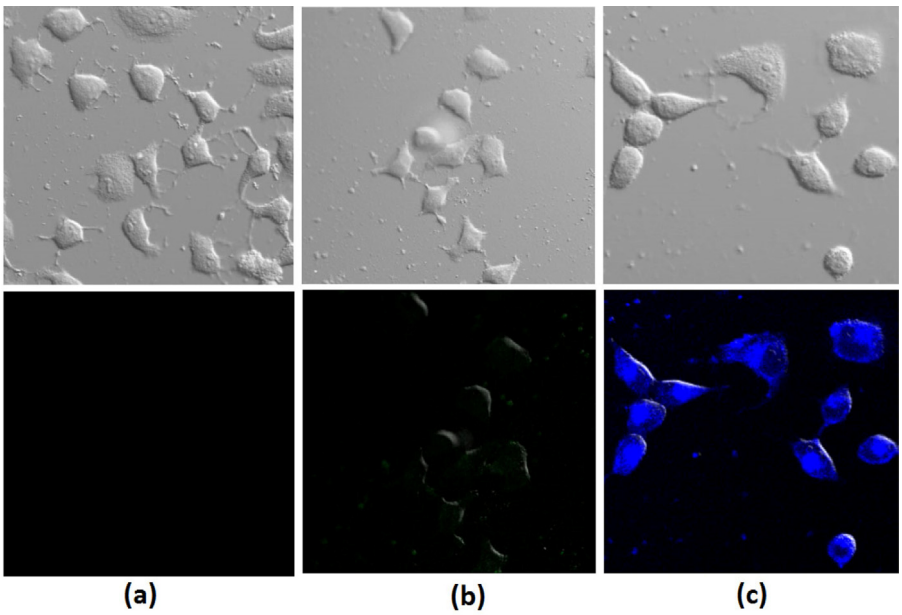

Fig. 12. Fluorescence microscopic images of MCF7 cells: (a) Untreated Cell control; (b) Cells treated with HL; (c) Cell treated with Zn^{2+} and HL.

than the keto form isomer, which suggests there might have an invertible structural conversion, i.e. the so-call ESIPT, which is consistent with the weak fluorescence of the probe.

Then we studied the Zn-L complex. We constructed two structures for the complex, one with two probe ligands (tetracoordination) and the other with two probe ligands and a coordinate water molecule (pentacoordination). As shown in Fig. S8 (supporting materials), the initial structure with pentacoordinate Zn was converted to a structure with a tetracoordinate Zn and a free water molecule. The results are consistent with above analysis on the recognition mechanism. In the following, we will focus on the structure with two deprotonated probe molecules and a tetracoordinate Zn (ZnL_2). As shown in Fig. 10, TD-DFT calculation at B3LYP/6-31G(d) level predicts the characteristic emission of ZnL_2 to be at 451 nm, which is very close to the experimentally recorded wavelength of 458 nm. Such an emission is dominated by the transition from HOMO excited state to corresponding LUMO (ratio = 98.8%) and the oscillator strength (f) is 0.867, indicating the very strong emission, which is consistent with the experimental results. Moreover, the detailed orbital analyses suggest that the characteristic emission of ZnL_2 is still originated by the individual ligand L and corresponds to the $\pi^* \rightarrow \pi$ transition (Fig. 10).

3.7. pH effects

To further demonstrate the proposed mechanism and evaluate the practical applicability of the probe, we examined the effect of pH to the emission of both mixed Zn-L system and the free probe HL in DMSO/HEPES buffer (v/v, 1:1). As shown in Fig. 11, in the acidic ($pH \leq 6$), neutral or weak alkali (pH = 7–9), and strong alkali ($pH \geq 10$) environments, the emissions of Zn-L mixed system would be very weak, considerably enhanced, and very strong, respectively. In the acidic environment, HL exists mainly in the stable protonated form and the ESIPT effect will lead to the weak fluorescence; in the neutral and weak alkali environment, HL exists mainly in the metastable protonated form and it is possible to form the Zn-L complex so that the fluorescence of corresponding probe ligands can be observed; while in the strong alkali environment, Zn^{2+} will binding with excess hydroxyl and almost all HL exists in deprotonated form to exhibit strong emission. Such reasoning can be proved by the similar studies on pH effect to the free probe HL, which shows weak emission for $pH \leq 8$, considerably enhanced emission at pH = 9, and almost same intensity to mixed Zn-L system for $pH \geq 10$. The results imply that the complexation of the probe with Zn^{2+} prevent the ESIPT process of the probe HL in the neutral or weak alkali environment. We also calculated the free deprotonated probe (L) to simulation the fluorescence in the strong alkali environment. As shown in Fig. 10, the predicted emission is at 501 nm, which is close to the experimental value of 485 nm. The *f* value is 0.636, which is consistent with the rather strong emission for L at strong alkali environment. The results of pH effects also demonstrate that the neutral or weak alkali environment are the most appropriate pH range for the probe to detect Zn^{2+}, which is preferred for the application in the physiological system.

3.8. Cell imaging study

Given the specific fluorescence response by the probe to Zn^{2+}, we measured the sensing performance of HL to Zn^{2+} in living cells by fluorescence microscopy. As shown in Fig. 12, the MCF7 cells incubated with the probe HL (10 μM) only show very weak green fluorescence image. In contrast, after incubation of the probe treated cells with Zn^{2+} (10 μM), the bright blue fluorescence is observed when the cells are imaged through the fluorescent microscope. The result reveals that the probe HL is cell-permeable and has potential applicability for detecting Zn^{2+} in living cells. We further studied the cytotoxicity using the MTT assay to evaluate the possibility of probe to be applied in the living cell. After the MCF7 cells were treated with the probe HL in the concentration range of 0 ~ 100 μM for 24 h, the cells showed very little decrease in viability (< 10%) (Fig. S9, supporting materials). The result indicates that the probe HL does not have any strong detrimental effect on cell viability and it could be considered to be low toxic.

4. Conclusion

In summary, we have successfully designed and synthesized a simple fluorescent probe which shows a good sensitivity and selectivity towards Zn^{2+} ion via 2:1 binding mode in DMSO/HEPES (v/v, 1:1). Upon binding with Zn^{2+}, the probe emits bright blue fluorescence. The enhancement of emission mainly originates from the inhibition of ESIPT process, while the selectivity toward Zn^{2+} is determined by the proper steric hindrance effect. The fluorescence mechanism of the probe HL toward Zn^{2+} was evaluated by ESI–MS, ^{1}HNMR and DFT computational studies. We also explored the potential applications to detect Zn^{2+} in biological systems. The low toxic probe was found to be cell membrane permeable and suitable for imaging Zn^{2+} in cultured MCF7 cells.

Acknowledgments

This work was supported financially by the Natural Science Foundation of China (NSFC, Grant Nos 21271121, 21273140, 21471092, and 21571118), the Special Program for Applied Research on Super Computation of the NSFC-Guangdong Joint Fund (the second phase), and the Program for the Innovative Talents of Higher Learning Institutions of Shanxi Province. The authors also thank Dr Zeng-Qiang Gao at line 3 W1A of BSRF for his help with the single-crystal X-ray diffraction data collection and reduction.

Appendix A. Supplementary data

Supplementary data associated with this article can be found, in the online version, at http://dx.doi.org/10.1016/j.snb.2016.09.149.

References

[1] C. Balakrishnan, M. Theetharappan, Satheesh Natarajan, S. Thalamuthua, M.A. Neelakantan, Fluorescence response of a thiazolidine carboxylic acid derivative for the selective and nanomolar detection of Zn(II) ions: quantum chemical calculations and application in real samples, RSC Adv. 5 (2015) 105453–105463.
[2] P.J. Fraker, L.E. King, Reprogramming of the immune system during zinc deficiency, Annu. Rev. Nutr. 24 (2004) 277–298.
[3] J.M. Berg, Y. Shi, The galvanization of biology: a growing appreciation for theroles of zinc, Science 271 (1996) 1081–1085.
[4] Z.-C. Xu, J.Y. Yoon, D.R. Spring, Fluorescent chemosensors for Zn^{2+}, Chem. Soc. Rev. 39 (2010) 1996–2006.
[5] A.P. de Silva, H.Q.N. Gunaratne, T. Gunnlaugsson, A.J.M. Huxley, C.P. McCoy, J.T. Rademacher, T.E. Rice, Signaling recognition events with fluorescent sensors and switches, Chem. Rev. 97 (1997) 1515–1566.
[6] B. Valeur, I. Leray, Design principles of fluorescent molecular sensors for cation recognition, Coord. Chem. Rev. 205 (2000) 3–40.
[7] J. Du, M. Hu, J. Fan, X. Peng, Fluorescent chemodosimeters using mild chemicalevents for the detection of small anions and cations in biological and environ-mental media, Chem. Soc. Rev. 41 (2012) 4511–4535.
[8] X. Chen, T. Pradhan, F. Wang, J.S. Kim, J. Yoon, Fluorescent chemosensors based on spiroring-opening of xanthenes and related derivatives, Chem. Rev. 112 (2012) 1910–1956.
[9] Y.L. Park, K.M.K. Swamy, J.Y. Yoon, Recent progress in fluorescent imaging probes, Sensors 15 (2015) 24374–24396.
[10] L.-J. Qu, C.-X. Yin, F.-J. Huo, J.-B. Chao, Y.-B. Zhang, F.-Q. Cheng, A pyridoxal-based dual chemosensor for visual detection of copper ion and ratiometric fluorescent detection of zinc ion, Sens. Actuators B Chem. 191 (2014) 158–164.
[11] M.-L. Chen, X. Lv, Y.-L. Liu, Y. Zhao, J. Liu, P. Wang, W. Guo, An 2-(2'-aminophenyl) benzoxazole- based OFF-ON fluorescent chemosensor for Zn^{2+} in aqueous solution, Org. Biomol. Chem. 9 (2011) 2345–2349.
[12] G.J. Park, H. Kim, J.J. Lee, Y.S. Kim, S.Y. Lee, S. Lee, I. Noh, C. Kim, A highly selective turn-on chemosensor capable of monitoring Zn^{2+} concentrations in living cells and aqueous solution, Sens. Actuators B Chem. 215 (2015) 568–576.
[13] J.-C. Qin, L. Fan, Z.-Y. Yang, A small-molecule and resumable two-photon fluorescent probe for Zn^{2+} based on a coumarin Schiff-bas, Sens. Actuators B Chem. 228 (2016) 156–161.
[14] Y.J. Na, I.H. Hwang, H.Y. Jo, S.A. Lee, G.J. Park, C. Kim, Fluorescent chemosensor based-on the combination of julolidine and furan for selective detection of zinc ion, Inorg. Chem. Commun. 35 (2013) 342–345.
[15] Y.-Q. Xu, L.-L. Xiao, S.-G. Sun, Z.-C. Pei, Y.-X. Pei, Y. Pang, Switchable and selective detection of Zn^{2+} or Cd^{2+} in living cells based on 3'-O-substituted arrangement of benzoxazole-derived fluorescent probes, Chem. Commun. 50 (2014) 7514–7516.
[16] A.N. Gusev, V.F. Shulgin, S.B. Meshkova, S.S. Smola, W. Linert, A novel triazole-based fluorescent chemosensor for Zinc ions, J. Lumin. 155 (2014) 311–316.
[17] M.M. Henary, Y. Wu, C.J. Fahrni, Zinc(II)-selective ratiometric fluorescent sensors based on inhibition of excited-state intramolecular proton transfer, Chem. Eur. J. 10 (2004) 3015–3025.
[18] T.-T. Zhang, F.-W. Wang, M.-M. Li, A simple pyrazoline-based fluorescent probe for Zn^{2+} in aqueous solution and imaging in living neuron cells, Sens. Actuators B Chem. 186 (2013) 755–760.
[19] Y. Sato, M. Yamada, S. Yoshida, T. Soneda, M. Ishikawa, T. Nizato, K. Suzuki, F. Konno, Benzoxazole derivatives as novel 5-HT3 receptor partial agonists in the gut, J. Med. Chem. 41 (1998) 3015–3021.
[20] K.R. Phatangare, B.N. Borse, V.S. Padalkar, V.S. Patil, V.D. Gupta, P.G. Umpae, N. Sekar, Synthesis, photophysical property study of novel fluorescent 4-(1,3-benzoxazol-2-yl)-2-phenylnaphtho[1,2-d][1,3] oxazole derivatives and their antimicrobial activity, J. Chem. Sci. 125 (2013) 141–151.
[21] H.A. Priestap, M.A. Barbieri, F. Johnson, Aristoxazole analogues. Conversion of 8-nitro-1-naphthoic acid to 2-methylnaphtho [1,2-d]oxazole-9-carboxylic acid: comments on the chemical mechanism of formation of DNA adducts by the aristolochic acids, J. Nat. Prod. 75 (2012) 1414–1418.
[22] J.F. Wang, W.H. Chen, X.M. Liu, C. Wesdemiotisa, Y. Pang, A mononuclear zinc complex for selective detection of diphosphate via ESIPT fluorescence turn-on, J. Mater. Chem. B 2 (2014) 3349–3354.
[23] L.-J. Tang, X. Dai, K.-L. Zhong, D. Wu, X. Wen, A novel 2,5-diphenyl-1,3,4-oxadiazole derived fluorescent sensor for highly selective and ratiometric recognition of Zn2+ in water through switching on ESIPT, Sens. Actuators B Chem. 203 (2014) 557–564.
[24] Z. Otwinowski, W. Minor, Processing of X-ray diffraction data collected in oscillation mode, Methods Enzymol. 276 (1997) 307–326.
[25] G.M. Sheldrick, SHELXS-97, Program for X-ray Crystal Structure Determination, University of Göttingen, Germany, 1997.
[26] C.-X. Yuan, X.-Y. Liu, Y.-B. Wu, L.-P. Lu, M.-L. Zhu, A triazole Schiff base-based selective and sensitive fluorescent probe for Zn^{2+}: A combined experimental and theoretical study, Spectrochim. Acta Part A 154 (2016) 215–219.
[27] C.-X. Yuan, L.-P. Lu, X.-L. Gao, Y.-B. Wu, M.-L. Guo. Y. Li, X.-Q. Fu, M.-L.Zhu Ternary oxovanadium(IV) complexes of ONO-donor Schiff base and polypyridyl derivatives as protein tyrosine phosphatase inhibitors: synthesis, characterization, and biological activities, J. Biol. Inorg. Chem. 14 (2009) 841–851.
[28] C.-X. Yuan, S.-F. Lan, L.-P. Lu, Evaluation of Cu(II) complexes with Schiff base of Salicylanilide as the inhibitiors of protein tyrosine phosphatases, Chin. J. Inorg. Chem. 31 (2015), 951–922.
[29] S.V. Aeken, J. Deblander, J.D. Houwer, T. Mosselmans, K.A. Tehrani, Unexpected reaction of 2-amino-1, 4-naphthoquinone with aldehydes: new synthesis of naphtho[2, 1-d]oxazole compounds, Tetrahedron 67 (2011) 512.
[30] A. Helal, S.H. Kim, H.-S. Kim, Thiazole sulfonamide based ratiometric fluorescent chemosensor with a large spectral shift for zinc sensing, Tetrahedron 66 (2010) 9925–9932.
[31] A. Helal, H.-S. Kim, Thiazole-based chemosensor: synthesis and ratiometric fluorescence sensing of zinc, Tetrahedron Lett. 50 (2009) 5510–5515.
[32] Q.J. Ma, X.B. Zhang, X.H. Zhao, Y.J. Gong, J. Tang, G.L. Shen, R.Q. Yu, A ratiometric fluorescent sensor for zinc ions based on covalently immobilized derivative of benzoxazole, Spectrochim. Acta Part A 73 (2009) 687–693.
[33] L.J. Tang, X. Dai, K.L. Zhong, X. Wen, D. Wu, A phenylbenzothiazole derived fluorescent sensor for Zn(II) recognition in aqueous solution through turn-on excited-state intramolecular proton transfer emission, J. Fluoresc. 24 (2014) 1487–1493.
[34] W.H. Ding, W. Cao, X.J. Zheng, W.J. Ding, J.P. Qiao, L.P. Jin, A tetrazole-based fluorescence turn-on sensor for Al (III) and Zn (II) ions and its application in bioimaging, Dalton Trans. 43 (2014) 6429–6435.
[35] J.H. Sun, Z. Liu, Y. Wang, S.H. Xiao, M.S. Pei, X.X. Zhao, G.Y. Zhang, A fluorescence chemosensor based on imidazo[1,2-a]quinoline for Al3+ and Zn2+ in respective solutions, RSC Adv. 5 (2015) 100873–100878.
[36] K. Tayade, S.K. Sahoo, B. Bondhopadhyay, V.K. Bhardwaj, N. Singh, A. Basu, R. Bendre, A. Kuwar, Highly selective turn-on fluorescent sensor for nanomolar detection of biologically important Zn^{2+} based on isonicotinohydrazide derivative: application incellularimaging, Biosens. Bioelectron. 61 (2014) 429–433.
[37] R.D. Shannon, Revised effective ionic radii and systematic studies of interatomic distances in halides and chalcogenides, Acta Crystallogr. A 32 (1976) 751–767.
[38] Q. Ma, M. Zhu, C. Yuan, S. Feng, L. Lu, Q. Wang, A molecular helix: self-assembly of coordination polymers from d^{10} metal ions and 1,10-phenanthroline-5,6-dione (pdon) with the bridges of SCN^- and Cl^- anions, Cryst. Growth Des. 10 (2010) 1706–1714.

Biographies

Caixia Yuan is an associate professor of the Institute of Molecular Science at Shanxi University, major in inorganic chemistry. Her current research interests are mainly in the development of chemosensors for metal ions and inorganic drugs.

Shiyang Li is currently pursuing a master degree at Shanxi University under the guidance of Prof. Cai-xia Yuan. Her study interests are the synthesis and characterization of organic luminescent molecules.

Yanbo Wu is a professor of the Institute of Molecular Science at Shanxi University, major in computational chemistry. His current research interests are mainly exploration of the reaction mechanism.

Liping Lu is a professor of the Institute of Molecular Science at Shanxi University, major in inorganic chemistry. Her current research interests are mainly in the development of inorganic drugs.

Miaoli Zhu is a professor of the Institute of Molecular Science at Shanxi University, major in inorganic chemistry. His current research interests are mainly in the development of multifunctional materials.